Chinese Journal of Natural Medicines

Anti-psoriasis molecular targets and active components discovery of *Optimized Yinxieling Formula* (OYF) via affinity-purified strategy

Wei Wang, Li-Juan Liu, Zhuo Yang, Chuan-Jian Lu, Peng-Fei Tu, Rui-Zhi Zhao, Ke-Wu Zeng

Citation: Wei Wang, Li-Juan Liu, Zhuo Yang, Chuan-Jian Lu, Peng-Fei Tu, Rui-Zhi Zhao, Ke-Wu Zeng, Anti-psoriasis molecular targets and active components discovery of *Optimized Yinxieling Formula* (OYF) via affinity-purified strategy, Chinese Journal of Natural Medicines, in press, 1-11. doi: 10.1016/S1875-5364(23)60516-3.

View online: https://doi.org/10.1016/S1875-5364(23)60516-3

Available online at www.sciencedirect.com
ScienceDirect
Chinese Journal of Natural Medicines 2024, **22**(2): 127-136
doi: 10.1016/S1875-5364(24)60563-7
Chinese Journal of Natural Medicines

•Original article•

Anti-psoriasis molecular targets and active components discovery of Optimized Yinxieling Formula *via* affinity-purified strategy

WANG Wei[1, 2], LIU Lijuan[2], YANG Zhuo[1], LU Chuanjian[2], TU Pengfei[1], ZHAO Ruizhi[2*], ZENG Kewu[1*]

[1] *State Key Laboratory of Natural and Biomimetic Drugs, School of Pharmaceutical Sciences, Peking University, Beijing 100191, China;*
[2] *State Key Laboratory of Dampness Syndrome of Chinese Medicine, The Second Affiliated Hospital of Guangzhou University of Chinese Medicine, Guangzhou 510006, China*

Available online 20 Jan., 2024

[ABSTRACT] Psoriasis, a prevalent inherited skin condition, involves an inflammatory response as a key pathogenic mechanism. The Optimized Yinxieling Formula (OYF), rooted in traditional Chinese medicine, is extensively utilized in clinical settings to treat psoriasis. Although previous studies have demonstrated OYF's significant anti-inflammatory effects in psoriasis, its potential molecular targets and active components remain unexplored. This study aimed to unveil the anti-psoriasis molecular targets and active components of OYF. Our findings indicated that OYF extract markedly reduced the production of several inflammatory mediators, including IL-23, nitric oxide, TNF-α, and IL-1β, in LPS-induced RAW264.7 cells. We synthesized OYF extract-crosslinked beads to isolate pharmacological targets from RAW264.7 lysates using an affinity purification strategy, known as Target Fishing. The enriched target proteins were subsequently identified *via* LC-MS/MS, followed by bioinformatics analysis to map the psoriasis-associated pathway-gene network. We identified a total of 76 potential target proteins, which were highly associated with mRNA transcription mechanisms. In particular, pathway-gene network analysis revealed that the IL-23 inflammatory pathway was involved in the anti-psoriasis effect of OYF extract. We further utilized a target protein-based affinity capture strategy, combined with LC-MS and SPR analysis, to globally screen OYF's active components, focusing on the mRNA transcription regulator, fused in sarcoma (FUS). This process led to the identification of umbelliferone, vanillic acid, protocatechuic acid, gentisic acid, and echinacoside as key compounds targeting FUS to inhibit IL-23 expression. Additionally, we formulated a compound cocktail (CpdC), which significantly reduced psoriasis area and severity index (PASI) scores and the expressions of IL-23 and Ki67 in an imiquimod (IMQ)-induced psoriasis mouse model. Collectively, our study elucidates the primary molecular targets and active components of OYF, offering novel insights for psoriasis treatment.

[KEY WORDS] Psoriasis; Optimized Yinxieling Formula (OYF); FUS protein; Molecular targets; Affinity-purified strategy.
[CLC Number] R965 **[Document code]** A **[Article ID]** 2095-6975(2024)02-0127-10

Introduction

Psoriasis, a chronic inflammatory skin condition, is characterized by well-defined erythematous plaques with silvery scales [1, 2]. Globally, it affects approximately 2% of the population, though prevalence rates vary regionally. The exact pathogenic mechanisms underlying psoriasis remain unclear [3], but current research suggests a complex interplay of genetic predisposition, environmental triggers, and innate immune responses [1, 4]. Despite the development and clinical use of several treatments, psoriasis remains incurable, significantly impacting patients' quality of life [5, 6]. Therefore, the identification of novel therapeutic targets and treatments for psoriasis is of paramount importance.

Psoriasis is an immune-mediated inflammatory skin disease. Currently, it has been indicated that macrophages contribute to the pathogenesis of psoriasis [7, 8]. Particularly, the macrophage-specific interleukin 23 (IL-23) immune signaling axis has been identified as a major molecular pathway in psoriasis pathogenesis [9]. Of note, macrophages serve as crucial contributors to the pathogenesis of psoriasis by produ-

[Received on] 19-Aug.-2023
[Research funding] This work was supported by the State Key Laboratory of Dampness Syndrome of Chinese Medicine, the Second Affiliated Hospital of Guangzhou University of Chinese Medicine (No. SZ2021ZZ51), the National Key R&D Program of China (No. 2022YFC3501601), the National Natural Sciences Foundation of China (Nos. 82174008 and 81973505), Jinan New 20 Policies for Higher Education Funding (No. 202228048) and the Fundamental Research Funds for the Central Universities.
[*]**Corresponding author]** E-mails: zhaoruizhi@gzucm.edu.cn (ZHAO Ruizhi); ZKW@bjmu.edu.cn (ZENG Kewu)
These authors have no conflict of interest to declare.

cing excessive IL-23 and other inflammation media [10-13]. Moreover, IL-23 promotes the proliferation of Th17 cells, which in turn secrete cytokines, such as IL-17, tumor necrosis factor-alpha (TNF-α), and IL-6 [10, 12, 14]. Meanwhile, these cytokines further induce the expression of psoriasis-related proteins from keratinocytes, leading to the development of epidermal hyperplasia, which represents a key pathological milestone of psoriasis [13, 15]. Therefore, dysfunction of macrophages plays a crucial role in psoriasis progression, warranting focused research.

In traditional Chinese medicine (TCM), the pathogenesis of psoriasis is closely associated with the dampness-heat stasis, which is one of the most common syndromes in TCM [16-18]. The Yinxieling Formula (YF), a time-honored traditional Chinese herbal formula, has been traditionally employed for psoriasis treatment due to its anti-inflammatory and immunoregulatory properties [19, 20]. The Optimized Yinxieling Formula (OYF), a modified version of YF, is now extensively used in clinical settings to treat psoriasis, with reports of reduced recurrence rates [21]. OYF is composed of Astragali Radix, Rehmanniae Radix, Smilacis glabrae Rhizoma, Atractylodis Macrocephalae Rhizoma, Curcumae Rhizoma, Paeoniae Radix Rubra, Trionycis Carapax, Mume Fructus, and Sarcandrae Herba (verified at http://www.theplantlist.org/). OYF has been reported to effectively counteract the dampness-heat stasis syndrome, thereby impeding the progression of psoriasis-like inflammation [21]. Moreover, OYF has been shown to inhibit the proliferation of lipopolysaccharide (LPS)-induced HaCaT keratinocytes and noticeably decreased the levels of TNF-α, IL-6, IL-1β, IL-17A, and IL-23 in the patients with psoriasis, signifying its substantial anti-inflammatory properties [21]. Meanwhile, OYF has been observed to markedly decrease TNF-α, IL-6, and IL-17A levels in a psoriasis mouse model [21]. Given the pivotal role of macrophage activation in psoriasis, our study primarily investigates the pharmacological effects of OYF in suppressing macrophage activation using an LPS-induced RAW264.7 cell model.

Despite these insights, the specific molecular targets and active components of OYF contributing to its anti-psoriatic effects remain unidentified. Our study thus aims to elucidate the pharmacological target proteins of OYF and clarify its anti-inflammatory mechanism in macrophages while identifying and screening the active components within OYF for anti-psoriasis efficacy.

Materials and Methods

Preparation of OYF extract

The ingredients for the OYF extract, including 30 g of Astragali Radix, 15 g of Rehmanniae Radix, 30 g of Smilacis glabrae Rhizoma, 15 g of Atractylodis Macrocephalae Rhizoma, 10 g of Curcumae Rhizoma, 15 g of Paeoniae Radix Rubra, 30 g of Trionycis Carapax, 15 g of Mume Fructus, and 15 g of Sarcandrae Herba were obtained from Guangdong Kangmei Pharmaceutical Company, and identified according to *Chinese Pharmacopoeia* (2020 edition). The preparation of OYF involved a traditional decoction method. Initially, the decoction pieces were soaked in water at ten times their volume for 30 min, followed by boiling for 1 h. The resultant decoction was then filtered, and the remaining residue underwent a second extraction. The combined filtrates were concentrated to yield a crude drug concentration of 0.5 mg·mL^{-1}. This concentrated solution was subsequently freeze-dried into a powder and stored at 4 °C for future use.

Chemicals and reagents

Umbelliferone ($C_9H_6O_3$), vanillic acid ($C_8H_8O_4$), and gentisic acid ($C_7H_6O_4$) were from Chengdu Must Bio-technology (Chengdu, China). Protocatechuic acid ($C_7H_4O_2$) was from Bidepharm (Shanghai, China). Echinacoside ($C_{35}H_{46}O_{20}$) was from Baoji Herbest Bio-Tech (Baoji, China). All compounds were affirmed by ^{1}H nuclear magnetic resonance (NMR) and mass spectrometry (MS) analysis. High-glucose Dulbecco's Modified Eagle Medium (DMEM), trypsin, penicillin-streptomycin, and phosphate buffer saline (PBS) were purchased from Macgene (Beijing, China). Fetal bovine serum (FBS) was obtained from PAN-Biotech (Aidenbach, Germany). LPS was obtained from Sigma-Aldrich (St Louis, MO, USA). Methylthiazolyldiphenyl-tetrazolium bromide (MTT), *E. coli* DH5α, *E. coli* BL21 (DE3), sodium chloride, yeast extract, peptone, HEPES, and imidazole were purchased from Solarbio (Beijing, China). MolPure Cell/Tissue Total RNA Kit, Hifair III 1st Strand cDNA Synthesis SuperMix, and Hieff qPCR SYBR Green Master Mix were obtained from Yeasen (Shanghai, China). Coomassie Protein Assay Reagent was from Thermo Fisher Scientific (Waltham, MA, USA). IMQ cream (5%) was purchased from Sichuan Mingxin Pharmaceutical (Chengdu, China). Methotrexate was purchased from Bidepharm (Shanghai, China). 4% Paraformaldehyde was obtained from Bioroyee Biotechnology (Beijing, China). Endogenous peroxidases blocker, goat serum albumin, and goat anti-rabbit secondary antibody were from ZSGB-Biotech (Beijing, China). The primary antibody against Ki67 was from Affinity Biosciences (Jiangsu, China), and that against IL-23 was from Bioss (Beijing, China).

Cell culture

Murine macrophages (RAW 264.7 cells), sourced from the Peking Union Medical College Cell Bank, Beijing, China, were cultured under controlled conditions. The cells were maintained in high-glucose DMEM supplemented with 10% FBS, 100 U·mL^{-1} penicillin, and 100 μg·mL^{-1} streptomycin at 37 ℃ in a humidified incubator with 5% CO_2 and 95% air.

MTT assay

RAW264.7 cells were treated with LPS (1 μg·mL^{-1}) in the presence or absence of OYF extract (100, 200, 400 μg·mL^{-1}). After 24 h, MTT solution (0.5 μg·mL^{-1}) was added to each well, followed by cell incubation for 4 h at 37 ℃. Then, the supernatant was removed, and 300 μL of dimethysulfoxide (DMSO) was added to each well to dissolve formazan crystals for 10 min at room temperature. The absorbance was then measured at 570 nm on a microplate read-

er (Tecan, Ausserfeld, Switzerland).

Nitric oxide (NO) assay

RAW264.7 cells were treated with LPS (1 μg·mL^{-1}) in the presence or absence of OYF extract (100, 200, 400 μg·mL^{-1}). After 24 h, the supernatant was collected for the NO assay using the NO assay kit (Jiancheng Bio-Engineering Institute, Nanjing, China). The procedure involved mixing equal volumes of the cell culture medium with Griess reagents I and II, followed by centrifugation to collect the supernatant. The supernatant was then reacted with Griess reagents III, IV, and V in a 96-well plate at room temperature for 10 min. The absorbance was measured at 570 nm using the same Tecan microplate reader.

RNA extraction and real-time PCR analysis

RAW264.7 cells were treated with LPS (1 μg·mL^{-1}) in the presence or absence of OYF extract (100, 200, 400 μg·mL^{-1}) for 6 h. Post-treatment, the cells were harvested, and total RNA was extracted using the MolPure Cell/Tissue Total RNA Kit (Yeasen, Shanghai, China), following the manufacturer's instructions. The extracted RNA was then reverse-transcribed to cDNA using the Hifair III 1st Strand cDNA Synthesis SuperMix for qPCR (Yeasen, Shanghai, China), *as per* the provided protocol. The resultant cDNA was diluted fivefold and subsequently subjected to PCR amplification using the Hieff qPCR SYBR Green Master Mix (Yeasen, Shanghai, China). The amplification protocol was set as follows: Initial denaturation at 98 °C for 10 min, followed by 40 cycles of denaturation at 98 °C for 30 s, annealing at 55 °C for 30 s, and elongation at 72 °C for 30 s. Glyceraldehyde 3-phosphate dehydrogenase (GAPDH) served as the internal control for normalization. The real-time PCR analysis provided the cycle threshold (CT) value for each reaction. The relative expression levels of the target genes, normalized to GAPDH, were calculated using the comparative $2^{-\Delta\Delta C_t}$ method. The primers used for real-time PCR are listed in Table 1.

Preparation of OYF extract photo-crosslinked beads

$FeCl_3·6H_2O$ (0.325 g) and Na_3Cit (0.20 g) were dissolved in ethylene glycol. $NaAc·3H_2O$ (1.20 g) was added to the mixture. Then, the mixture was reacted at 200 ℃ for 8 h. Racemic-2-3-dimercaptosuccinic acid (15 mg) was added to the product and shaken for 1.2 h to synthesize sulfhydryl-bound Fe_3O_4 beads. Next, ethyl ester L-lysine triisocyanate (44.5 mg) and 4,4′-dihydroxybenzophenone (42.8 mg) were added to sulfhydryl-bound Fe_3O_4 beads to synthesize 4,4′-dihydroxybenzophenone (DHBP)-bound Fe_3O_4 beads. OYF extract powder (5 mg) was dissolved in water (200 μL). Then, the solution was added to methanol (20 mL) with DHBP-bound Fe_3O_4 beads (5 mg). OYF extract and DHBP-bound Fe_3O_4 beads were mixed and irradiated under UV (254−365 nm) at 25 ℃ for 1 h to produce OYF extract-crosslinked beads.

Table 1 Primer pairs for real-time PCR.

Gene	Sequence
IL-23	F: 5′-TGGAGCAACTTCACACCTCC-3′
	R: 5′-GGCAGCTATGGCCAAAAAGG-3′
TNF-α	F: 5′-AAGCAAGCAGCCAACCAG-3′
	R: 5′-CCACAAGCAGGAATGAGAAGA-3′
IL-1β	F: 5′-TGGAGAAGCTGTGGCAGCTACCT-3′
	R: 5′-GAACGTCACACACCAGCAGGTT-3′
GAPDH	F: 5′-GGTGAAGGTCGGTGTGAACG-3′
	R: 5′-CTCGCTCCTGGAAGATGGTG-3′

Target protein identification using affinity-purified strategy (Target Fishing)

RAW264.7 cells were treated with LPS (1 μg·mL^{-1}) for 1 h and lysed with Lysis Buffer containing 1% NP-40. OYF extract-crosslinked beads were then mixed with cell lysates for incubation overnight at 4 ℃. Meanwhile, OYF extract (400 μg·mL^{-1}) was added to one group of lysates for competitive binding with target proteins. The proteins captured from the lysates were eluted and digested with trypsin. The resulting peptides were then analyzed using liquid chromatography with an LTQ Velos pro mass spectrometer (Waltham, MA, USA).

Liquid chromatography coupled to tandem MS (LC-MS/MS) analysis of target proteins

The trypsin-digested samples were loaded on a trapping column filled with 5 μm C_{18} reversed-phase material. The C_{18} reversed-phase material column (75 μm × 10 cm, 3 μm particle size) was used for the chromatographic separation of peptides. The program of gradient elution was as follows: 2%−40% B for 70 min; 40%−95% B for 5 min; 95% B for 20 min (solvent A: 0.1% formic acid in water, solvent B: 0.1% formic acid in ACN). Then, the eluent was brought into the mass spectrometer at a flow rate of 300 nL·min^{-1}. Parameters included a resolution of 60 000, a maximum ion trap (IT) time of 50 ms, and scan spectra ranging from *m/z* 350 to 2000. The target false discovery rate (FDR) for peptide-spectrum matches (PSMs) was set to 0.01, with a higher-energy collisional dissociation (HCD) collision energy of 35%. Proteome MS data was analyzed by Proteome Discover (1.4) software with the SEQUEST search engine (Thermo Scientific).

Recombinant FUS protein expression and purification

The DNA sequence encoding FUS was cloned into the *NdeI/XhoI* restriction sites of the modified pet28a vector with His-tag. The plasmid was transformed into *E. coli* BL21 (DE3) cells. These cells were cultured in a medium (2 L) and incubated at 37 ℃ and 220 r·min^{-1} until OD600 reached 0.6. Then, the cells were induced with 1 mmol·L^{-1} isopropyl *β*-D-thiogalactopyranoside (IPTG) at 16 ℃ for 18 h to produce recombinant FUS proteins. Subsequently, the cells were collected and lysed in lysis buffer (20 mmol·L^{-1} HEPES, 250 mmol·L^{-1} NaCl, 10 mmol·L^{-1} imidazole). The proteins were purified using Ni-NTA resin (GE Healthcare, Chicago, IL, USA) with HEPES buffer (20 mmol·L^{-1} HEPES, 250 mmol·L^{-1} NaCl, 10−250 mmol·L^{-1} imidazole). The purity of

the proteins was confirmed by Coomassie's brilliant blue staining. Finally, the proteins were concentrated by centrifugation at 4000 r·min^{-1} in an ultrafiltration tube (Millipore, Waltham, MA, USA) and dissolved in PBS buffer.

Screening of active compounds from OYF extract

Ni beads were mixed with recombinant FUS proteins to facilitate binding at 4 ℃. Then, the beads were washed with 0.5% triton in PBS. The FUS-bound beads were mixed with OYF extract (200 μg·mL^{-1}) and incubated for 6 h at 4 ℃. The beads-captured compounds from OYF extract were eluted with 0.1% trifluoroacetic acid (500 μL) and lyophilized at −45 ℃. These compounds were dissolved in 10% acetonitrile and analyzed by LC-MS/MS, employing both negative and positive ion modes.

LC-MS/MS analysis of compounds

The dissolved sample was chromatographically separated on Waters ACQUITY UPLC HSS T3 1.8 μm, 2.1 mm × 100 mm column, VanGuard Pre-Column HSS T3, 2.1 mm × 5 mm, 1.8 μm (Thermo Vanquish F). Subsequently, the eluent was introduced into the mass spectrometer. The parameters of MS were set to DDA, Top20, with a full MS range from 100 to 1000 *m/z*, and NCE set at 25/35/45 (Thermo Q Exactive HF-X). MS data were analyzed using Xcalibur software (Thermo Scientific).

Surface plasmon resonance (SPR) assay

Interactions between nine compounds and FUS were quantitatively analyzed using the Biacore T200 system (GE Healthcare, Boston, USA). The recombinant FUS (500 μg·mL^{-1}) was immobilized on a carboxymethylated five-sensor chip using the standard amine coupling method. The analytes, consisting of nine compounds at gradient concentrations ranging from 0.39 to 200 μmol·L^{-1}, were introduced in a running buffer (Tris-HCl 50 mmol·L^{-1}, pH 7.2, 100 mmol·L^{-1} KCl). Data were analyzed using the Biacore evaluation software (T200 Version 2.0), and the dissociation constant (K_D) was obtained by fitting the data to a 1∶1 Langmuir binding model.

Animal study

Experimental procedures were approved by the Ethical Institution Animal Care and Use Committee of Peking University (EIACUC-PKU, No. LA2023158), Beijing, China. All study procedures adhered to *International Ethical Guidelines* and the *National Institutes of Health Guide*. Male BALB/c mice (6−8 weeks, 18−22 g) were obtained from Vital River Laboratories (Beijing, China). The mice were housed in a controlled at 25 ± 1 ℃ with a 12 h dark/12 h light cycle. They had free access to food and water and underwent a 7-day acclimation. Then, the mice were randomly divided into four groups, each consisting of eight mice: the control group, IMQ-induced model group, compound cocktail group (CpdC, 40 mg·kg^{-1}), and methotrexate group (MTX, positive control, 1 mg·kg^{-1}). The hair on the dorsal surface of mice was cut on the day before the experiment (hairless area: 2 cm × 3 cm). Mice in the control and model groups were given 0.5% CMC-Na by oral gavage daily. The remaining groups were administered their respective treatments. Two hours post-administration, the mice in the control group were smeared with 62.5 mg vaseline, while the mice in other groups were smeared with 62.5 mg IMQ on the back skin every day. Treatments were carried out for seven consecutive days. On the 8th day, the mice were euthanized, and the severity of psoriasis on their back skin was evaluated using the Clinical Psoriasis Area and Severity Index (PASI). Erythema, scaling, and thickening were independently scored as follows: 0, none; 1, slight; 2, moderate; 3, marked; and 4, very marked. The cumulative score, summing erythema, scaling, and thickening, ranged from 0 to 12, reflecting the overall severity of inflammation.

Immunohistochemistry (IHC) analysis

Skin tissue samples were fixed with 4% paraformaldehyde solution for at least 24 h. The fixed tissues were then embedded in paraffin and sectioned into slices approximately 5 μm thick using a microtome. Antigen retrieval for these sections was conducted in a microwave for 10 min. Post-retrieval, the sections were washed with PBS and treated with H_2O_2 for 10 min to inhibit endogenous peroxidase activity. Subsequently, 5% goat serum albumin was applied to the sections, followed by 30-min incubation. The sections were incubated with primary rabbit anti-mouse Ki67 antibody (1∶200) or with primary rabbit anti-mouse IL-23 antibody (1∶200) overnight at 4 ℃, followed by incubation with the goat anti-rabbit secondary antibody for 20 min at 37 ℃. Detection was accomplished using a 3-3′-diaminobenzidine (DAB) substrate kit (ZSGB-Biotech, Beijing, China). The sections were counterstained with hematoxylin. The sections were examined using a WS-10 Digital Panoramic Scanner (Zhiyue, Jiangsu, China), and the immunostaining intensity was quantified using the Image-J.

Statistical analysis

All experiments were performed at least three times. Statistical analysis was performed using one-way analysis of variance (ANOVA) with GraphPad Prism 8.0 software. All data were expressed as mean ± standard error of the mean (SEM). A P value of less than 0.05 was considered statistically significant.

Results

OYF extract inhibited macrophage-mediated inflammation response

To investigate the anti-inflammatory effect of OYF during psoriasis development, we examined the effect of OYF extract on LPS-induced inflammatory mediator production in RAW264.7 cells. An initial MTT assay was conducted to assess the potential cytotoxicity of the OYF extract. The results indicated that LPS treatment did not affect the viability of RAW264.7 cells. Similarly, OYF extract exhibited no significant cytotoxicity at concentrations of 100, 200, and 400 μg·mL^{-1} (Fig. 1A). As shown in Fig. 1B, further investigation revealed that LPS markedly stimulated the release of NO from RAW264.7 cells. However, this effect was significantly mitigated by OYF extract in a concentration-dependent manner. Given the critical role of IL-23, TNF-α, and IL-1β as inflammatory mediators released by macrophages in psorias-

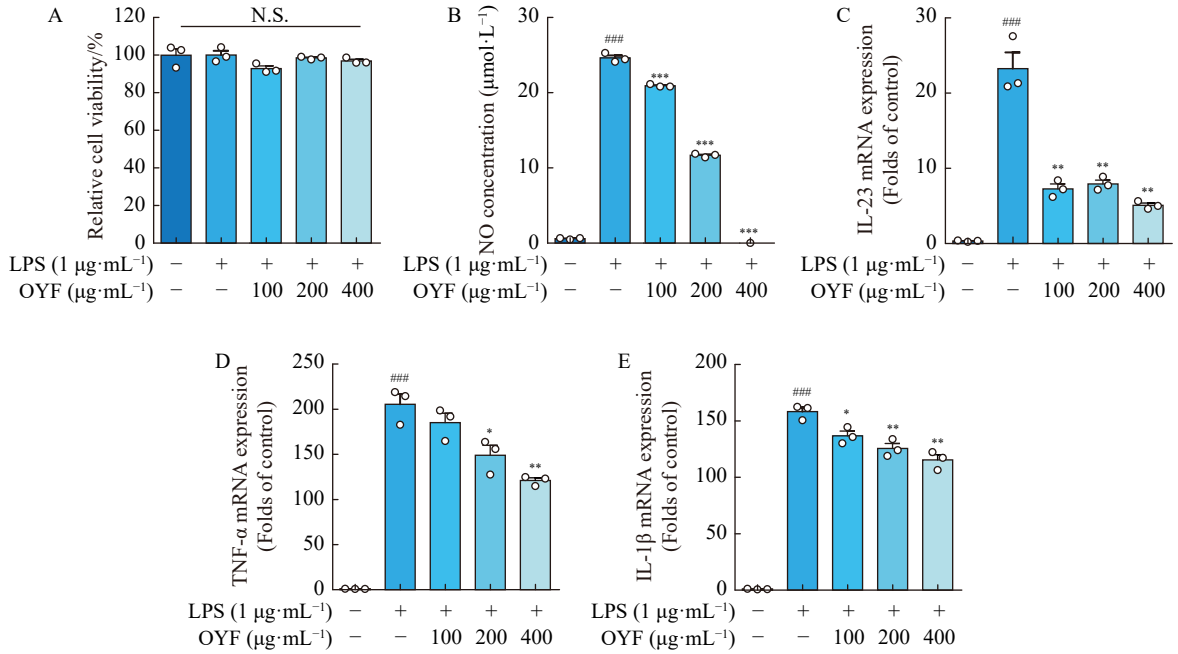

Fig. 1 OYF extract inhibited macrophage-mediated inflammation response in LPS-induced RAW264.7 cells. (A) LPS (1 μg·mL^{-1}) with or without OYF (100, 200 and 400 μg·mL^{-1}) did not affect cell viability. (B) OYF inhibited LPS-induced NO production in RAW264.7 cells. (C−E) OYF inhibited LPS-induced IL-23 (C), TNF-α (D), and IL-1β (E) mRNA expressions in RAW264.7 cells. Bars represent mean ± SEM of three independent experiments, two-tailed unpaired Student's *t* test, $^{*}P < 0.05$, $^{**}P < 0.01$, $^{***}P < 0.001$ *vs* LPS group; $^{\#\#\#}P < 0.001$ *vs* control group; N.S., not significant by ANOVA with Dunnett's *post-hoc* test.

is pathogenesis, the study also examined the impact of OYF extract on the mRNA expression of these mediators. The findings indicated that LPS significantly induced the mRNA expression of IL-23, TNF-α, and IL-1β in RAW264.7 cells. Notably, OYF extract effectively reduced the expression of these mediators in a concentration-dependent manner (Figs. 1C−1E). In summary, the results demonstrate that OYF extract substantially inhibits the inflammatory response mediated by macrophages in psoriasis.

Identification of molecular targets of OYF extract via affinity-purified strategy (Target Fishing)

To explore the pharmacological mechanism of OYF against macrophage-mediated inflammation in psoriasis, we attempted to identify the direct molecular targets of OYF extract in macrophages. Here, we prepared OYF extract-crosslinked beads *via* UV-induced crosslinking reaction (ZY strategy) as previously described [22]. Then, the OYF extract-crosslinked beads were incubated with RAW264.7 cell lysates in the presence or absence of OYF extract for competition. The OYF extract-captured proteins were eluted from beads, followed by tryptic digestion into peptides. The resultant peptides were routinely analyzed by LC-MS/MS (Fig. 2A). We identified a total of 71 potential target proteins as presented by the volcano scatter plot (Fig. 2C). Among these, FUS, OTUD4, Nono, PSA1, and SAFB1 were closely associated with inflammation progress. Moreover, gene enrichment analysis was performed using the Metascape platform, including GO Biological Processes, KEGG Pathway, Reactome Gene Sets, and Wiki Pathways. Terms with a *P*-value < 0.01, a minimum count of 3, and an enrichment factor > 1.5 were collected. The filtered entries were displayed in a bar graph with the bar length representing the $-\log_{10}(P)$ value of terms (Fig. 2B). We found that the most significant pathways were associated with mRNA processing and mRNA surveillance. The proteins in mRNA processing consisted of FUS, Nono, Pspc1, Sfpq, Ddx1, Ewsr1, Hnrnpl, and Rbmx. Meanwhile, the proteins in the mRNA surveillance pathway included FUS, Ppp1c, Rnmt, and Nudt21. These observations indicate that FUS plays a central role in OYF-mediated inflammation progress. Further exploration of signaling pathways was performed using KEGG analysis with Cytoscape. We found that there were two crucial signaling pathways involved in the pathway-gene network, including the mRNA surveillance pathway and spliceosome (Fig. 2D). In particular, FUS also played a crucial role in the two pathways, which may represent an essential molecular target of OYF.

Global screening of FUS-binding components from OYF extract

In light of the critical role of FUS in the anti-inflammatory effects of OYF on macrophages, the study aimed to identify potential FUS-binding components within the OYF extract. To achieve this, recombinant FUS protein-crosslinked Ni beads were prepared. The OYF extract was then incubated with these beads to capture FUS-binding compounds. The components bound to the beads were eluted and subsequently analyzed using LC-MS/MS in both negative and positive ion modes. This analysis led to the identification of nine compounds: protocatechuic acid, gentisic acid, umbelliferone, vanillic acid, atractylodes III, formononetin, calycosin, calycosin glycoside, and echinacoside (Fig. 3A). Next, we

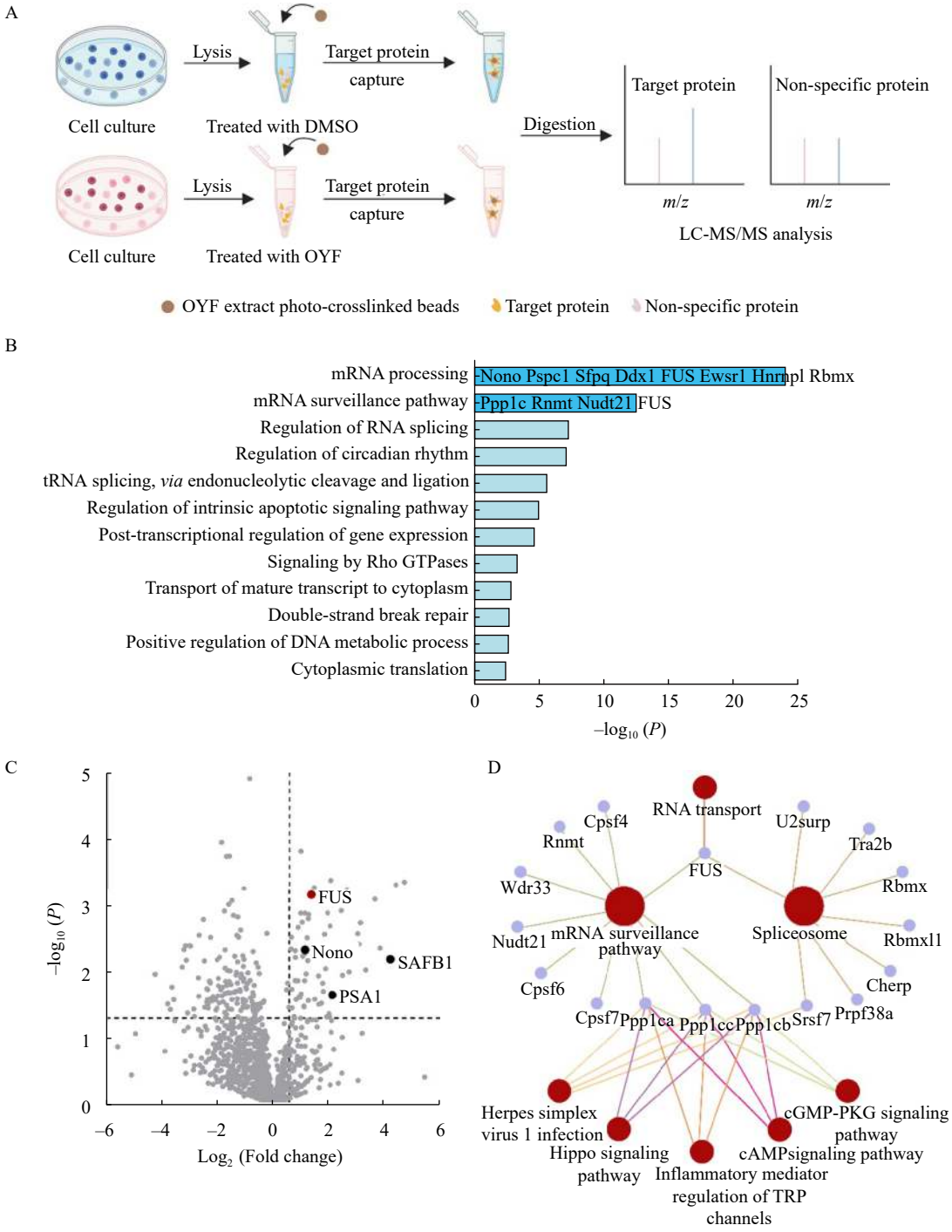

Fig. 2 Identification of molecular targets of OYF extract *via* affinity-purified strategy (Target Fishing). (A) Workflow of pull-down/MS-based target identification of OYF. (B) Target profiles of OYF extract were shown by a scattered plot. *X*-axis: protein level difference indicated by $\log_2$ (fold change), *Y*-axis: statistical significance indicated by $-\log_{10}$ (*P*). (C) Enrichment terms for analysis of potential targets on Metascape. (D) The pathway-gene network analysis on Cytoscape.

performed SPR analysis to verify the direct interaction between these compounds and FUS. The SPR data indicated strong binding affinities of umbelliferone and echinacoside to FUS, with equilibrium dissociation constant (K_d) values of 4.76×10^{-6} and 7.62×10^{-7} mol·L^{-1}, respectively. Meanwhile, the medium binding ability of protocatechuic acid, vanillic acid, gentisic acid, formononetin, and calycosin with FUS was also confirmed by the K_D values of 1.19×10^{-5}, 2.09×10^{-5}, 2.68×10^{-5}, 4.06×10^{-5}, and 2.83×10^{-5} mol·L^{-1}, respectively (Fig. 3B). Our observations suggest that these compounds may be the potential active components. Since IL-23 is a major inflammatory mediator involved in the macrophage-specific pathogenesis of psoriasis, we then analyzed the effects of these compounds on LPS-induced IL-23 levels.

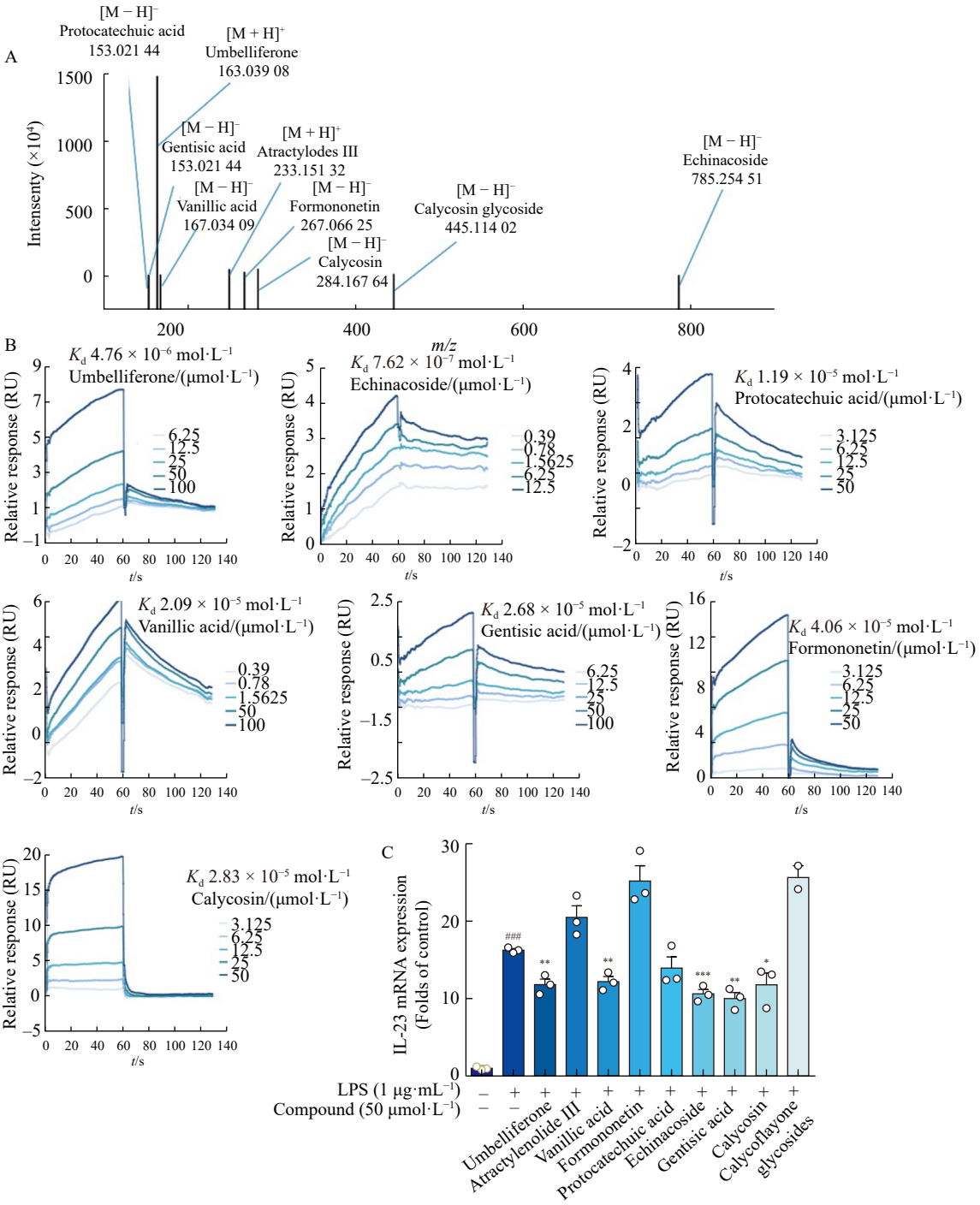

Fig. 3 Global screening of FUS-binding components from OYF extract. (A) A total of 9 compounds binding to FUS were detected by LC-MS/MS. (B) The target affinities of 9 compounds binding to FUS were detected by SPR analysis. (C) The effects of 9 compounds on LPS-induced IL-23 levels in macrophages were determined by real-time PCR analysis. Bars represent mean ± SEM of three independent experiments, two-tailed unpaired Student's *t*-test, $^{*}P < 0.05$, $^{**}P < 0.01$, $^{***}P < 0.001$ *vs* LPS group; $^{\#\#\#}P < 0.001$ *vs* control group; N.S., not significant by ANOVA with Dunnett's *post-hoc* test.

As shown in Fig. 3C, LPS significantly induced IL-23 production, which was inhibited by umbelliferone, vanillic acid, protocatechuic acid, gentisic acid, echinacoside, and calycosin. Thus, we speculated that these compounds might serve as the major active components of OYF extract, contributing to its anti-psoriasis effect.

Active CpdC protects skin lesions of IMQ-induced psoriasis in mice

Since several FUS-binding components were identified for potential anti-inflammatory effects in psoriasis, we then prepared a CpdC by combining the major bioactive molecules, including umbelliferone, vanillic acid, protocat-

echuic acid, gentisic acid, and echinacoside, in equal proportions with a ratio of 1 ∶ 1 ∶ 1 ∶ 1. To investigate the therapeutic capacity of CpdC on psoriasis, we established an IMQ-induced psoriasis model of BALB/c mice. Compared with the control group, the skin of mice in the IMQ group appeared erythema, scaling, and thickening; however, CpdC significantly reversed these typical pathological features in the IMQ-induced mice, similar to MTX (positive control) (Fig. 4A). Moreover, the mice in IMQ group showed increased PASI scores, which were notably reduced in CpdC group (Fig. 4B).

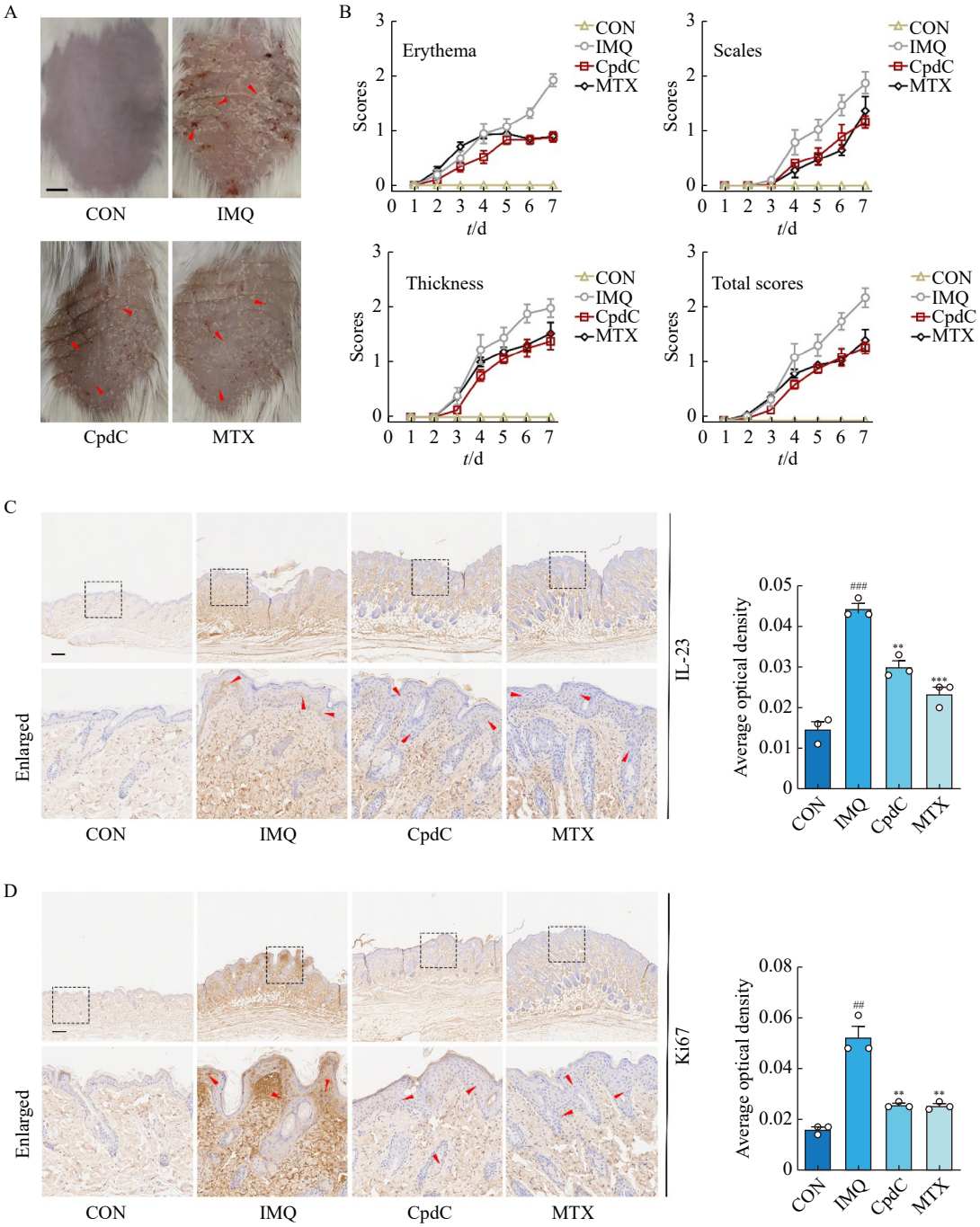

Fig. 4 CpdC protected skin lesion of IMQ-induced psoriasis in mice. (A) Images from each group after the 7th day of modeling (scale bar = 5 mm). Arrows indicate the typical pathological condition of back skin in mice. (B) PASI scores in the control, model, CpdC (40 mg·kg^{-1}) and MTX (positive control, 1 mg·kg^{-1}) treated mice. (C) IHC analysis of IL-23 expression in each group of mice (scale bar = 400 μm). Arrows indicate the high expression of IL-23. (D) IHC analysis of Ki67 expression in each group of mice (scale bar = 400 μm). Arrows indicate the high expression of Ki67. Bars represent mean ± SEM of three independent experiments, two-tailed unpaired Student's *t*-test, $^{**}P < 0.01$, $^{***}P < 0.001$ *vs* IMQ group; $^{\#\#}P < 0.01$, $^{\#\#\#}P < 0.001$ *vs* control group; N.S., not significant by ANOVA with Dunnett's *post-hoc* test.

To further evaluate the improvement effect of CpdC in IMQ-induced pathological changes of skin tissues, we conducted IHC analysis in the skin samples of mice. We found that the expressions of Ki67 and IL-23 were evidently increased with the treatment of IMQ (Figs. 4C and 4D); however, CpdC treatment significantly reversed IMQ-induced increase of Ki67 and IL-23 in skin tissues (Figs. 4C and 4D). These data suggest that CpdC, embodying the major active constituents of the OYF extract, effectively inhibits the inflammatory response triggered by IMQ and subsequently reduced the proliferation of keratinocytes during psoriasis.

Discussion

Psoriasis is a crucial immune-mediated inflammatory skin disease. In recent years, cytokine inhibitors have been verified to produce curative effects on psoriasis. and some have been approved for the treatment of psoriasis, such as IL-23 inhibitor tildrakizumab, TNF-α inhibitor certolizumab, and IL-17 inhibitor ixekizumab [23-27]. These agents have demonstrated efficacy, yet their long-term use raises concerns about potential side effects, a common issue in chronic disease management [28, 29]. Consequently, there is an ongoing search for more effective and safer therapeutic options. Traditional Chinese herbal medicine offers a rich source of potential treatments for immunological diseases, such as rheumatoid arthritis, allergy, and chronic primary immune thrombocytopenia [30-32]. Notably, these herbal remedies have shown long-term curative effects on psoriasis, characterized by widespread clinical application and lower side effects [22, 33, 34]. As a traditional herbal prescription, YF significantly decreases the levels of PASI, TNF-α, and IL-8 in psoriasis patients [35]. OYF is an optimized edition of YF, which is currently used for the treatment of psoriasis with more effective curative effects and low recurrent rates [21]. Despite its clinical success, a comprehensive understanding of the pharmacological targets and active components of OYF in psoriasis therapy has been lacking.

The identification of molecular targets is a crucial step in elucidating the pharmacological mechanisms of traditional medicine. In this study, we adopted an affinity-purified strategy to isolate direct target proteins of OYF extract [22]. This involved the use of Fe_3O_4 beads bound with a photosensitive chemical group (diphenylketone), which exhibited a well-dispersed and regular spherical shape. Under UV light, diphenylketone transforms into a carbon radical (carbene), enabling the covalent binding of plant extracts. Here, the chemical components of OYF extract were photochemically crosslinked onto the surface of beads *via* a UV crosslinking reaction that was mediated by a photoinitiator for capturing the target proteins from macrophage cell lysates (target proteins library). This technique is suitable for complex molecular systems such as traditional medicine. It is important to note that some identified proteins are highly associated with inflammation responses. In particular, FUS enhances NF-κB-mediated transactivation that is induced by inflammation and motivates the expression of inflammatory factors, which promotes the progression of psoriasis [36, 37]. FUS is also known to regulate circular RNA (circRNA) expression, contributing to the progression of psoriasis [38]. Other identified proteins, such as Nono, Pspc1, and Sfpq, have been reported to activate the innate immune response through the cGAS-STING pathway [39]. Our study also revealed that OYF's anti-psoriasis effects were largely mediated through the regulation of mRNA transcription, which was supported by the multifunctional role of FUS in RNA transcription regulation and alternative splicing [40, 41]. Thus, FUS may represent a major molecular target of OYF extract for the anti-psoriasis effect.

We identified key active compounds in OYF extract, including umbelliferone, vanillic acid, protocatechuic acid, gentisic acid, and echinacoside. Umbelliferone and protocatechuic acid are the main active components of the traditional Chinese medicine *Atractylodes macrocephala* Koidz. Vanillic acid, gentisic acid, and echinacoside are the main components of *Paeonia veitchii* Lynch, Fructus Mume, and *Rehmannia glutinosa*. Previous research has established that these components mainly exhibit anti-inflammatory and antioxidant properties [42-46]. The formulated CpdC, comprising these active constituents, demonstrated significant protective effects in an IMQ-induced mouse model of psoriasis, indicating that CpdC may serve as a promising modern agent from traditional prescription in psoriasis therapy. Notably, the precise composition and defined quality control of CpdC enhance its potential for translational medicine applications. One of the key advantages of CpdC is the low concentration of each compound, which reduces the likelihood of serious side effects, addressing a critical concern in current psoriasis treatments. This aspect is particularly beneficial for the advancement of anti-psoriatic drug development in clinical settings.

In conclusion, this study elucidates the pharmacological targets and active components of OYF extract, contributing significantly to our understanding of its mechanism of action against psoriasis. The discovery of these active compounds from OYF not only validates the therapeutic potential of traditional medicine but also paves the way for novel clinical agent development for psoriasis treatment.

References

[1] Chiricozzi A, Romanelli P, Volpe E, *et al*. Scanning the immunopathogenesis of psoriasis [J]. *Int J Mol Sci*, 2018, **19**(1): 179.
[2] Tang YZ, Yu JY, Zhao W, *et al*. Total glucosides of Rhizoma Smilacis Glabrae: a therapeutic approach for psoriasis by regulating Th17/Treg balance [J]. *Chin J Nat Med*, 2023, **21**(8): 589-598.
[3] Rendon A, Schäkel K. Psoriasis pathogenesis and treatment [J]. *Int J Mol Sci*, 2019, **20**(6): 1475.
[4] Schäkel K, Schön MP, Ghoreschi K. Pathogenesis of psoriasis [J]. *Hautarzt*, 2016, **67**(6): 422-431.
[5] Reid C, Griffiths CEM. Psoriasis and treatment: past, present and future aspects [J]. *Acta Derm Venereol*, 2020, **100**(3): adv00032.
[6] Kim WB, Jerome D, Yeung J. Diagnosis and management of psoriasis [J]. *Can Fam Physician*, 2017, **63**(4): 278-285.
[7] Wang Y, Edelmayer R, Wetter J, *et al*. Monocytes/macrophages play a pathogenic role in IL-23 mediated psoriasis-like skin inflammation [J]. *Sci Rep*, 2019, **9**(1): 5310.
[8] Hou Y, Zhu L, Tian H, *et al*. IL-23-induced macrophage polarization and its pathological roles in mice with imiquimod-in-

duced psoriasis [J]. *Protein Cell*, 2018, **9**(12): 1027-1038.
[9] Girolomoni G, Strohal R, Puig L, *et al*. The role of IL-23 and the IL-23/T_H 17 immune axis in the pathogenesis and treatment of psoriasis [J]. *J Eur Acad Dermatol Venereol*, 2017, **31**(10): 1616-1626.
[10] Vičić M, Kaštelan M, Brajac I, *et al*. Current concepts of psoriasis immunopathogenesis [J]. *Int J Mol Sci*, 2021, **22**(21): 11574.
[11] Kamata M, Tada Y. Dendritic cells and macrophages in the pathogenesis of psoriasis [J]. *Front Immunol*, 2022, **13**: 941071.
[12] Xiong DK, Shi X, Han MM, *et al*. The regulatory mechanism and potential application of IL-23 in autoimmune diseases [J]. *Front Pharmacol*, 2022, **13**: 982238.
[13] Tan Z, Lin ZJ, Wu LJ, *et al*. The macrophage IL-23/IL-17A pathway: a new neuro-immune mechanism in female mechanical pain [J]. *Neurosci Bull*, 2022, **38**(4): 453-455.
[14] Hawkes JE, Yan BY, Chan TC, *et al*. Discovery of the IL-23/IL-17 signaling pathway and the treatment of psoriasis [J]. *J Immunol*, 2018, **201**(6): 1605-1613.
[15] Coimbra S, Figueiredo A, Castro E, *et al*. The roles of cells and cytokines in the pathogenesis of psoriasis [J]. *Int J Dermatol*, 2012, **51**(4): 389-395.
[16] Song C, Yang C, Meng S, *et al*. Deciphering the mechanism of Fang-Ji-Di-Huang-Decoction in ameliorating psoriasis-like skin inflammation *via* the inhibition of IL-23/Th17 cell axis [J]. *J Ethnopharmacol*, 2021, **281**: 114571.
[17] Meng S, Lin Z, Wang Y, *et al*. Psoriasis therapy by Chinese medicine and modern agents [J]. *Chin Med*, 2018, **13**: 16.
[18] Wei RL, Li ZR, Cao RD, *et al*. New analysis of Banxia Xiexin Decoction and its similar prescriptions in treatise on febrile diseases to explore the universality of the treatment and compatibility principle [J]. *WJTCM*, 2022, **8**(4): 509-513.
[19] Xu M, Deng J, Xu K, *et al*. In-depth serum proteomics reveals biomarkers of psoriasis severity and response to traditional Chinese medicine [J]. *Theranostics*, 2019, **9**(9): 2475-2488.
[20] Yao DN, Lu CJ, Wen ZH, *et al*. Comparison of PSORI-CM01 granules and Yinxieling Tablets for patients with chronic plaque psoriasis: a pilot study for a randomized, double-blinded, double-dummy, multicentre trial [J]. *Ann Palliat Med*, 2021, **10**(2): 2036-2047.
[21] Xiang CL. *Integrated Network Pharmacology and Metabolomics to Explain Possible Mechanisms of Gu-Ben-Qu-Shi-Hua-Yu Decoction for Treating Psoriasis* [D]. Guangzhou University of Chinese Medicine, 2021.
[22] Zhao M, Yao L, Zhang X, *et al*. Global identification of the cellular targets for a multi-molecule system by a photochemically-induced coupling reaction [J]. *Chem Commun (Camb)*, 2021, **57**(28): 3449-3452.
[23] Li T, Gao S, Han W, *et al*. Potential effects and mechanisms of Chinese herbal medicine in the treatment of psoriasis [J]. *J Ethnopharmacol*, 2022, **294**: 115275.
[24] Parab S, Doshi G. An update on emerging immunological targets and their inhibitors in the treatment of psoriasis [J]. *Int Immunopharmacol*, 2022, **113**(Pt A): 109341.
[25] Yang K, Oak ASW, Elewski BE. Use of IL-23 inhibitors for the treatment of plaque psoriasis and psoriatic arthritis: a comprehensive review [J]. *Am J Clin Dermatol*, 2021, **22**(2): 173-192.
[26] Yu K, Yu X, Cao S, *et al*. Layered dissolving microneedles as a need-based delivery system to simultaneously alleviate skin and joint lesions in psoriatic arthritis [J]. *Acta Pharm Sin B*, 2021, **11**(2): 505-519.
[27] Chen Y, Li K, Jiao M, *et al*. Reprogrammed siTNFα/neutrophil cytopharmaceuticals targeting inflamed joints for rheumatoid arthritis therapy [J]. *Acta Pharm Sin B*, 2023, **13**(2): 787-803.
[28] Altenburg A, Augustin M, Zouboulis CC. Side effects of biologic therapies in psoriasis [J]. *Hautarzt*, 2018, **69**(4): 290-297.
[29] Armstrong AW, Read C. Pathophysiology, clinical presentation, and treatment of psoriasis: a review [J]. *JAMA*, 2020, **323**(19): 1945-1960.
[30] Wang Y, Chen S, Du K, *et al*. Traditional herbal medicine: therapeutic potential in rheumatoid arthritis [J]. *J Ethnopharmacol*, 2021, **279**: 114368.
[31] Ma HD, Deng YR, Tian Z, *et al*. Traditional Chinese medicine and immune regulation [J]. *Clin Rev Allergy Immunol*, 2013, **44**(3): 229-241.
[32] Liu WB, Li S, Yu XL, *et al*. Research progress on Chinese medicine immunomodulatory intervention for chronic primary immune thrombocytopenia: targeting cellular immunity [J]. *Chin J Integr Med*, 2019, **25**(7): 483-489.
[33] Lu CJ, Yu JJ, Deng JW. Disease-syndrome combination clinical study of psoriasis: present status, advantages, and prospects [J]. *Chin J Integr Med*, 2012, **18**(3): 166-171.
[34] Herman A, Herman AP. Topically used herbal products for the treatment of psoriasis: mechanism of action, drug delivery, clinical studies [J]. *Planta Med*, 2016, **82**(17): 1447-1455.
[35] Dai YJ, Li YY, Zeng HM, *et al*. Effect of Yinxieling Decoction on PASI, TNF-α and IL-8 in patients with psoriasis vulgaris [J]. *Asian Pac J Trop Med*, 2014, **7**(8): 668-670.
[36] Uranishi H, Tetsuka T, Yamashita M, *et al*. Involvement of the pro-oncoprotein TLS (translocated in liposarcoma) in nuclear factor-kappa B p65-mediated transcription as a coactivator [J]. *J Biol Chem*, 2001, **276**(16): 13395-1401.
[37] Han G, Li X, Wen CH, *et al*. FUS contributes to nerve injury-induced nociceptive hypersensitivity by activating NF-κB pathway in primary sensory neurons [J]. *J Neurosci*, 2023, **43**(7): 1267-1278.
[38] Zhang C, Han X, Yang L, *et al*. Circular RNA *circPPM1F* modulates M1 macrophage activation and pancreatic islet inflammation in type 1 diabetes mellitus [J]. *Theranostics*, 2020, **10**(24): 10908-10924.
[39] Morchikh M, Cribier A, Raffel R, *et al*. HEXIM1 and NEAT1 long non-coding RNA form a multi-subunit complex that regulates DNA-mediated innate immune response [J]. *Mol Cell*, 2017, **67**(3): 387-399.e5.
[40] Yang L, Gal J, Chen J, *et al*. Self-assembled FUS binds active chromatin and regulates gene transcription [J]. *Proc Natl Acad Sci U S A*, 2014, **111**(50): 17809-17814.
[41] Xue YC, Ng CS, Mohamud Y, *et al*. FUS/TLS suppresses enterovirus replication and promotes antiviral innate immune responses [J]. *J Virol*, 2021, **95**(12): e00304-e00321.
[42] Wang D, Wang X, Tong W, *et al*. Umbelliferone alleviates lipopolysaccharide-induced inflammatory responses in acute lung injury by down-regulating TLR4/MyD88/NF-κB signaling [J]. *Inflammation*, 2019, **42**(2): 440-448.
[43] Zhang RX, Li MX, Jia ZP. *Rehmannia glutinosa*: review of botany, chemistry and pharmacology [J]. *J Ethnopharmacol*, 2008, **117**(2): 199-214.
[44] Li J, Yu H, Yang C, *et al*. Therapeutic potential and molecular mechanisms of echinacoside in neurodegenerative diseases [J]. *Front Pharmacol*, 2022, **13**: 841110.
[45] Calixto-Campos C, Carvalho TT, Hohmann MS, *et al*. Vanillic acid inhibits inflammatory pain by inhibiting neutrophil recruitment, oxidative stress, cytokine production, and NF-κB activation in Mice [J]. *J Nat Prod*, 2015, **78**(8): 1799-1808.
[46] Liu Z, Peng Y, Ma P, *et al*. An integrated strategy for anti-inflammatory quality markers screening of traditional Chinese herbal medicine Mume Fructus based on phytochemical analysis and anti-colitis activity [J]. *Phytomedicine*, 2022, **99**: 154002.

Cite this article as: WANG Wei, LIU Lijuan, YANG Zhuo, LU Chuanjian, TU Pengfei, ZHAO Ruizhi, ZENG Kewu. Anti-psoriasis molecular targets and active components discovery of Optimized Yinxieling Formula *via* affinity-purified strategy [J]. *Chin J Nat Med*, 2024, **22**(2): 127-136.